



Regular Article

Removal of Phosphate from the Aqueous Environment Using Iron Oxide/Activated Carbon Composites: Activated Carbon Derived from Ziziphus Nuts as a New Precursor

B. Mousazadeh¹, N. Mohammadi¹, T. Hamoule^{2*}

¹ Department of Gas Engineering, Petroleum University of Technology, Ahvaz, Iran

² Department of Basic Science, Petroleum University of Technology, Ahvaz, Iran

ARTICLE INFO

Article history:

Received: 2021-11-17

Accepted: 2022-02-06

Available online: 2022-04-21

Keywords:

Adsorption,
Magnetic Adsorbent,
Phosphate,
Activated Carbon,
Ziziphus Nuts

ABSTRACT

Ziziphus nuts are abundant in Khuzestan province, Iran, and are considered as an unwanted natural biomass waste. The present study is aimed to develop low-cost activated carbon from Ziziphus nuts as a new precursor for the removal of phosphate from the water environment. The iron oxide modification was performed to simultaneously facilitate the adsorbent separation via a simple magnetic process and increase the phosphate removal capacity. The iron oxide/activated carbon composite (IOAC) was characterized using XRD, EDX, SEM, and BET methods. The specific surface area for IOAC reached 569.41 m²/g, comparable to that of the commercial activated carbon. While other similar derived-from-biomasses activated carbon reached the phosphate removal capacity of around 15 mg/g, IOAC demonstrated the excellent phosphate removal performance of as high as 27 mg/g. Also, IOAC showed fast adsorption kinetics, achieving equilibrium in only 60 minutes. According to the results, the pseudo-second-order kinetic model was more consistent with the data related to the phosphate adsorption onto the adsorbent than the pseudo-first-order model. The adsorption results using Langmuir, Freundlich, and Webber-Morris diffusion models were interpreting. The maximum Langmuir adsorption capacity was calculated to be 27 mg/L. The adsorbent was removed from the aqueous solution via a simple magnetic process.

DOI: 10.22034/ijche.2022.315429.1415 URL: http://www.ijche.com/article_144893.html

1. Introduction

In recent decades, the entry of industrial and agricultural runoffs into nature, mainly water

bodies such as rivers, lakes, and seas, has been one of the major environmental concerns [1]. As the main origins of phosphate

*Corresponding author: t.hamoule@put.ac.ir (T. Hamoule)

contamination, these sources have negatively affected the water quality and aquatic organisms [2]. The concentration of phosphorous exceeding its permissible limits causes eutrophication [3]. It promotes the fast growth of the marine plants, particularly algae, which leads to the reduction of the content of the dissolved oxygen and eventually the extinction of living organisms in the water environment [4]. In order to control the health of the aquatic environment, the concentration of phosphate must be maintained in the range of 0.010-0.100 mg P/L for rivers and 0.005-0.050 mg P/L for lakes and water supplies [5].

There are several potential strategies, such as the treatment using chemicals, biological treatment, and physical methods, for the removal of phosphate from water [6]. Biological methods have shown remarkable capabilities to eliminate phosphate while they are less effective at the lower concentrations of phosphate [7]. Physical methods such as reverse osmosis and electrodialysis are not appropriate due to their high cost and inefficiency [8]. In addition, chemical methods such as chemical precipitation are not promising because of their cost issue and generating toxic byproducts [9, 10]. Adsorption-based separation methods, however, have been stood out as promising approaches for removing phosphate from aqueous environments due to their cost-effectiveness, effortless operation, and high removal performance [11].

Adsorbent materials being the core building block of the adsorption process, determine the feasibility of the whole process. Many research groups have studied numerous materials, such as metal oxides, metal-organic frameworks, zeolites, and activated carbon, as the adsorbents for the removal of

contaminants [12-15]. Although some of these materials have shown high adsorption capacities, there are major challenges, such as high cost, difficult synthesis methods, and recovery processes, preventing them from being used at large scales [9]. In order to overcome these challenges, activated carbon can be identified as an ideal candidate because of its properties, including the porous structure, large surface area, simple preparation and lower cost [16]. Activated carbon can be produced via a simple pyrolysis process and from a wide range of raw materials such as orange peels, nutshell, and sugar beet tailings [17-19]. However, it still has a significant drawback, which is the low capacity of the uptake of phosphate. Also, the activated carbon derived from the derivatives of biomasses are present as powders, making the separation of adsorbent difficult [20].

Integrating metal oxides within the activated carbon pores network has been proved to increase the capacity of the phosphate adsorption. Modifying activated carbon using MgO and AlOOH was an effective approach to enhance the phosphate removal performance [20]. The modification of activated carbon nanofibers by iron oxide and zirconium oxide simultaneously was an efficient method to prepare effective adsorbents for the removal phosphorous from natural waters [21]. Zhang's research group also used lanthanum oxide loaded activated carbon fibers to remove phosphate from wastewater. Loading magnetic medium also significantly facilitates the adsorbent separation via a simple magnetic process [22].

The objective of the current study is to produce low-cost iron oxide/activated carbon composites as magnetic adsorbents based on Ziziphus nuts as a new raw material. Critical experimental parameters, including the initial

concentration of phosphate, initial pH of the solution, adsorbent dosage, and contact time, influencing the phosphate adsorption capacity were investigated via batch adsorption experiments. The physiochemical properties of the adsorbent were investigated using XRD, EDX, SEM and BET methods.

2. Methods

2.1. Chemical reagents

Chemical reagents which were used through the experiments were purchased from local commercial suppliers and were of analytical grade. Ziziphus nuts were collected from the local places in Ahvaz, Iran. The collected nuts were washed, oven-dried, grinded and stored for further use.

2.2. Production of activated carbon (AC)

The production of activated carbon from Ziziphus nuts was carried out following a typical one-step chemical activation-pyrolysis process. Ziziphus nuts and ZnCl₂ with the mass ratio of 1:2 were mixed in 50 mL deionized water and agitated for 24 h. Then, the solution was filtered, and in order to remove the water content, the solid material was put in the oven at 110 °C for 24 h. The chemical activation-pyrolysis process was

carried out using a horizontal tubular furnace. The solid material was placed in the furnace and was carbonized under an inert atmosphere of the nitrogen gas flow (200 cm³/min) at 600 °C for one h. The obtained product was repeatedly subjected to washing with cold and hot deionized water. Eventually, the product was dehumidified at 110 °C for 24 h under atmospheric conditions.

2.3. Preparation of iron oxide/activated carbon composites (IOAC)

A simple method was followed to prepare the iron oxide/activated carbon (IOAC) adsorbent. Briefly, 3.24 g of FeCl₃ and 1.26 g of FeCl₂ were mixed in 100 mL deionized water. Then, 4 g of previously prepared AC was added to the mixture and stirred for 30 min at 70 °C. Afterwards, a 5 mol/L NaOH solution was added dropwise to the solution until a black precipitate was formed (in approximately 30 min). The obtained precipitate was filtered and repeatedly subjected to washing with a 50 % ethanol:water solution to remove impurities. Finally, the obtained product was dried at 80 °C under atmospheric conditions for 4 h. The preparation process of IOAC is schematically showed in Figure 1.

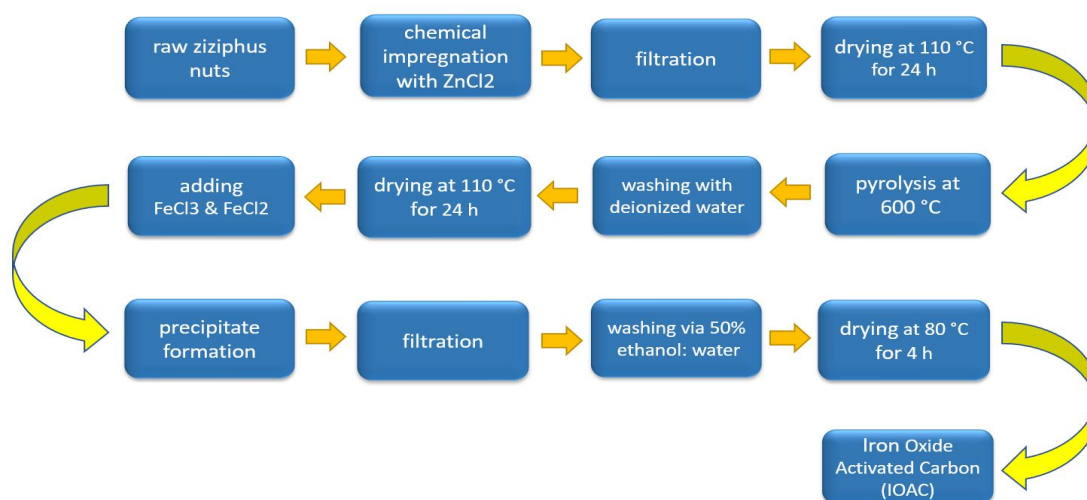


Figure 1. Schematic illustration of the preparation process of IOAC.

2.4. Adsorption procedure

Batch adsorption experiments were performed to study the adsorption of phosphate onto IOAC. Briefly, a certain dose of the adsorbent was introduced to the phosphate solution of a known concentration, and the solution was stirred for 24 h to reach equilibrium. Next, the adsorbent was removed from the mixture using a magnet, and the equilibrium concentration of phosphate was measured by a UV-VIS spectrometer. The adsorbent removal process is schematically shown in

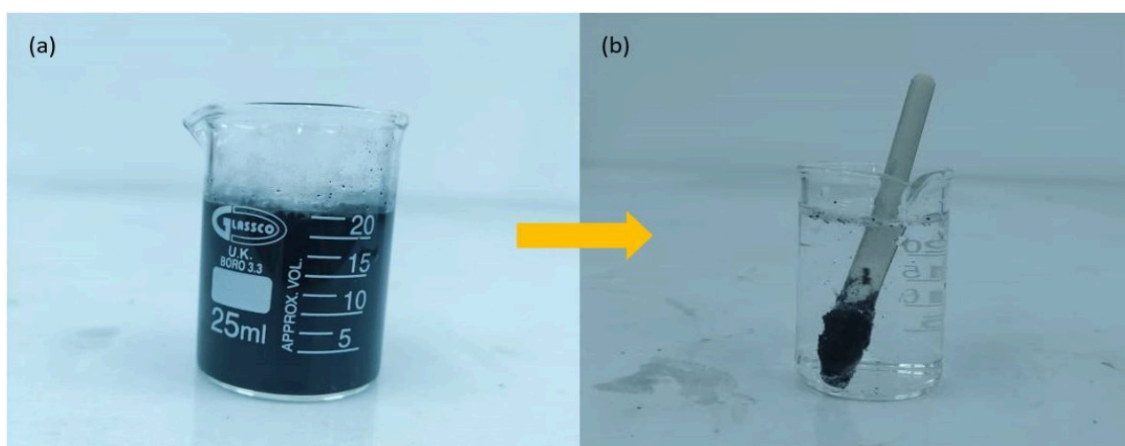


Figure 1. Schematic illustration of the adsorbent separation process, (a) the experiment sample including the adsorbent, (b) the adsorbent collected using a magnet.

3. Results and discussion

3.1. Characterization

3.1.1. XRD

The X-ray diffraction spectra of IOAC are shown in Figure 3. There are some characteristic peaks of magnetite in the XRD spectra of IOAC. More precisely, the diffraction peaks of 30.3, 36, 43.55, 53.9, 57.4 and 63.1 are attributed to the magnetite [23]. Also, there are some peaks below the 2θ of 26, which usually originate from carbon and the graphitic structure. The obtained XRD pattern of IOAC is consistent with the literature [23].

3.1.2. EDX

The electron dispersive X-ray analysis was

performed to explore the elemental composition of IOAC, which is recorded in Figure 4. The existence of iron and oxygen confirms the formation of magnetite. Also, there are some peaks related to the presence of carbon, calcium, sodium, and sulfur where Ca, Na, and S exist as impurities.

$$q_e = \frac{(c_0 - c_e)v}{m} \quad (1)$$

where q_e is the phosphate adsorption capacity (mg P/g adsorbent), v is the volume of the solution (L), m is the adsorbent dosage (g), c_e is the equilibrium concentration of phosphate (mg P/L), and c_0 is the initial concentration of phosphate (mg P/L).

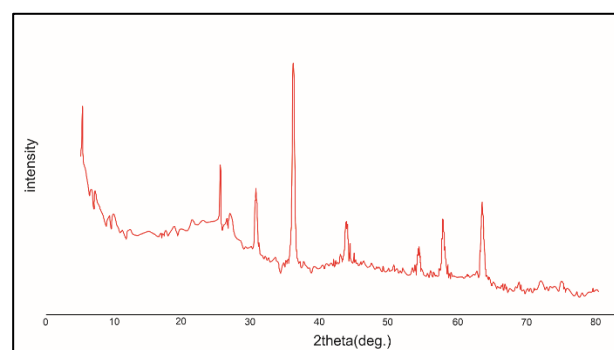


Figure 2. XRD pattern of IOAC.

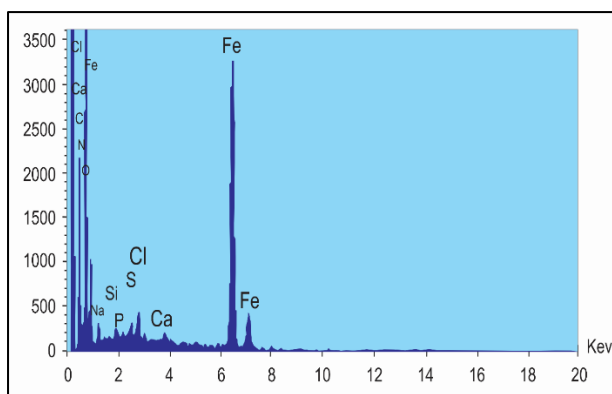


Figure 3. EDX pattern of IOAC.

3.1.3. SEM

SEM images are provided to obtain information about the morphology of IOAC. As it can be seen from the SEM images, irregular pore networks with different sizes and structures were formed. The presence of white particles is attributed to the formation of magnetite crystals. Some cubic shapes can be observed as the characteristics of magnetite particles.

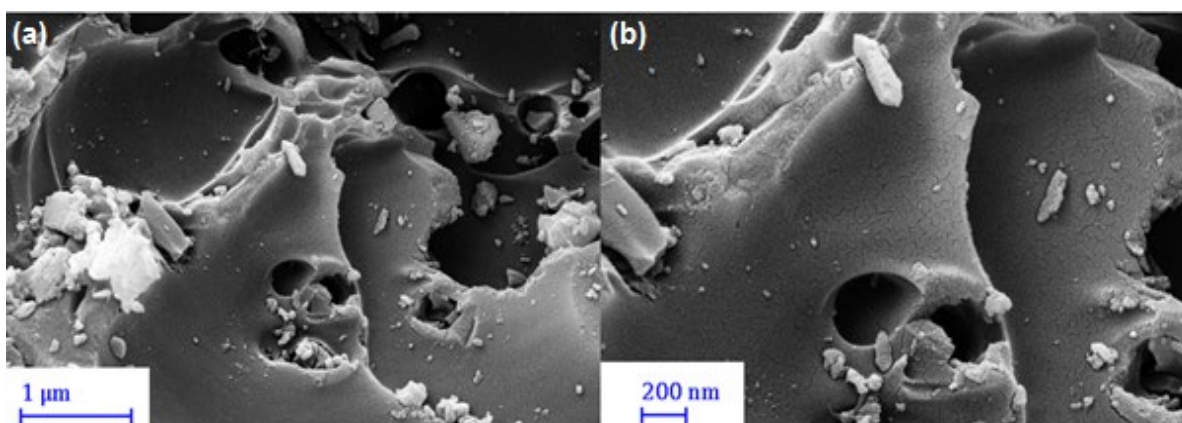


Figure 4. (a) SEM images of IOAC (1 μm), (b) SEM image of IOAC (200 nm).

3.1.4. BET

The N₂ adsorption-desorption isotherm and the corresponding pore size distribution data are provided in Figure 6. According to the IUPAC classification, the isotherm may be assigned as type IV. Textural parameters of IOAC such as the specific surface area (S_{BET}), average pore diameter (APD) and total pore volume (V_{pore}) are presented in Table 1. From Figure 6, it is clear that the adsorption of

nitrogen molecules mainly occurs in the low-pressure region ($p/p_0 < 0.2$) indicating the presence of narrow pores, particularly micropores. Also, an increase in the N₂ adsorption capacity at the relative pressures of above 0.2 reveals the existence of mesopores and some macropores. However, the pore size distribution plot clearly shows that the structure of IOAC is dominated by micropores.

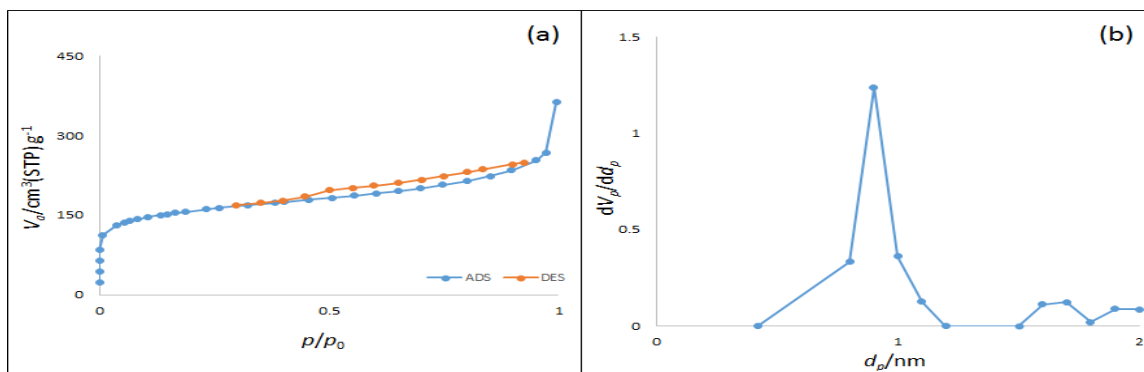


Figure 5. (a) N₂ adsorption-desorption isotherm of IOAC, (b) the pore size distribution of IOAC.

Table 1

Textural parameters of IOAC.

Adsorbent	S _{BET} (m ² /g)	Total pore volume (cm ³ /g)	Average pore width (°A)
IOAC	569.41	0.26	12.3

3.1.5. pH_{pzc}

The point of the zero charge of IOAC was measured using the procedure described earlier [24]. Briefly, several solutions were prepared at different pH values varying between 2 and 10. Next, 0.5 g of IOAC was introduced to 25 mL of each solution and sealed while nitrogen atmosphere inside. The final pH of each solution was measured after 24 h, and the final pH vs. the initial pH was plotted in Figure 7. The pH_{pzc} was taken as the pH value at which the final and initial pH values were equal. The pH_{pzc} was obtained to be 6.8.

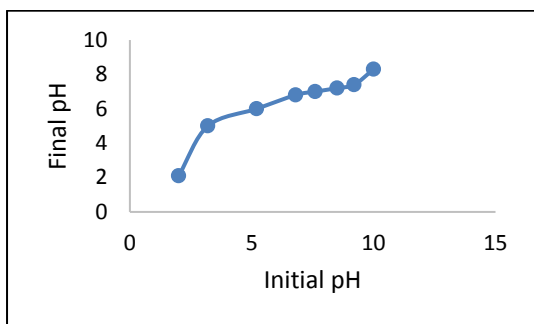


Figure 6. Final pH vs. the initial pH of the solution containing IOAC.

3.1.6. Adsorbent dosage

From an economic perspective, the amount of the adsorbent used for the process is of significant importance. In large-scale applications, the cost of adsorbents as the core factor of the process almost determines the economic feasibility of the whole process. Therefore, optimizing the adsorbent dosage contributes remarkably to the reduction of the cost. For this purpose, different adsorbent dosages were introduced to 50 mL of a 30 mg P/L phosphate solution. The contact time of 24 h was maintained to ensure equilibrium.

The result of the adsorbent is recorded in Figure 8. Increasing the amount of the adsorbent resulted in the enhancement of the uptake of phosphate due to the increased availability of adsorption sites. It was observed that there was a negligible increase in the uptake of phosphate at the larger amounts of the adsorbent. Therefore, an adsorbent dose of 2 g/L was chosen as the optimum amount. The optimum adsorbent dose is used for the rest of the study.

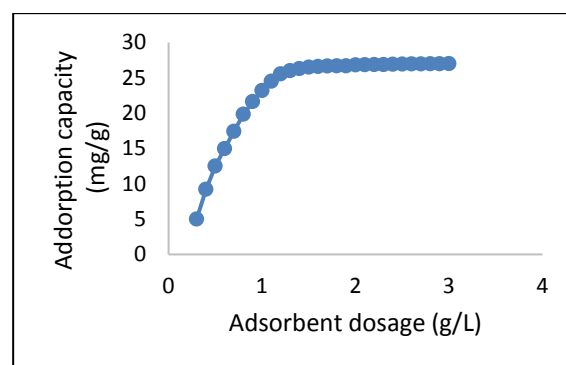


Figure 7. Effect of the IOAC dosage on the phosphate adsorption capacity.

3.1.7. pH effect

In order to optimally use the adsorbent and economically save, the initial pH of the solution should be properly adjusted. Previous studies have proved that the initial pH of the solution has a notable impact on the surface charge of the adsorbent. Also, various forms of phosphate at different pH values consequently influence the capacity of the uptake of phosphate. The effect of pH was investigated under conditions where the adsorbent dosage was 2 g/L, phosphate concentration was 30 mg P/L, and pH value was within the range of 2-10. The result is shown in Figure 9. As it is clear from this

figure, the adsorption of phosphate onto IOAC is highly pH-dependant. At pH values smaller than pH_{pzc} ($pH_{pzc}=6.8$), the adsorption of phosphate is more because the surface of the adsorbent becomes positively charged, which benefits the adsorption of phosphate particles. However, the adsorption capacity dramatically falls by increasing the pH values to larger than pH_{pzc} . It may be due to the electrostatic repulsion and competition between OH^- ions and phosphate particles [25].

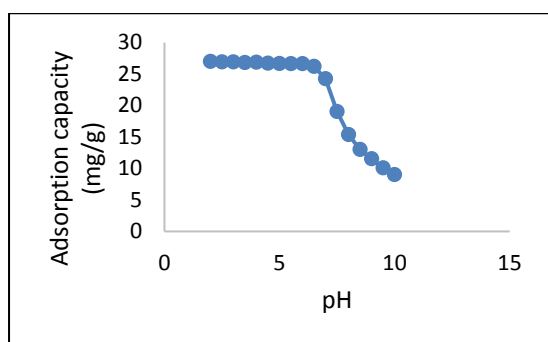


Figure 8. Effect of the initial pH of the solution on the capacity of the adsorption of phosphate onto IOAC.

3.1.8. Contact time

The equilibrium time is a significant parameter determining the applicability of the adsorbent for the industrial use. In order to probe the effect of time on the uptake of phosphate onto IOAC two kinetic pseudo-first-order and pseudo-second-order models were investigated. For this purpose, 2 g/L of IOAC was introduced to 50 mL of the phosphate solution containing 30 mg of P/L,

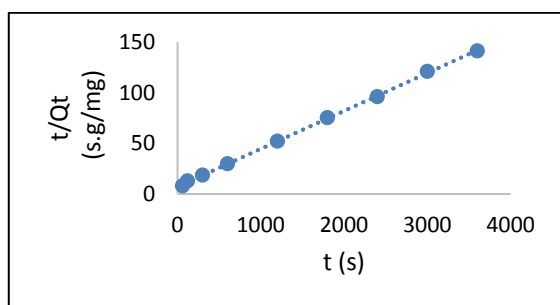


Figure 9. Pseudo-second-order model plot.

and constant sampling was performed at different time intervals until no change was observed in the adsorption capacity. The corresponding kinetic data plots and calculated parameters are recorded in Figure 10, Figure 11 and Table 2 respectively. The corresponding equations are as follows:

$$\ln(Q_e - Q_t) = \ln Q_e - k_1 t \quad (2)$$

$$\frac{t}{Q_t} = \frac{t}{k_2 Q_e^2} + \frac{t}{Q_e} \quad (3)$$

where Q_e is the amount of the adsorption of phosphate per one gram of the adsorbent after the equilibrium time (mg/g), Q_t is the amount of the removal of phosphate per one gram of the adsorbent after the time of t (mg/g), k_1 is the constant parameter of the pseudo-first-order equation (1/min), k_2 is the constant parameter of the pseudo-second-order equation (g/mg min). It was observed that the adsorption of phosphate on IOAC reached equilibrium in approximately 1 h. This fast adsorption kinetics shows the superior performance of the prepared adsorbent. The pseudo-second-order model was found better describing the removal of phosphate using IOAC because the R^2 value obtained for the pseudo-second-order model was larger than that for the pseudo-first-order model. Also, the theoretical adsorption capacity (Q_e) calculated from the pseudo-second-order plot was close to the actual experimental value ($Q_{\text{experimental}} = 26.6 \text{ mg P/g}$).

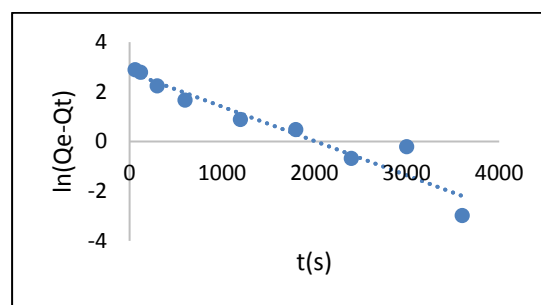


Figure 10. Pseudo-first-order model plot.

Table 2

Fitting variables obtained from the pseudo-first-order and pseudo-second-order models.

Pseudo-first-order			Pseudo-second-order		
k_1 (1/s)	Q_e (mg/g)	R_1^2	k_2	Q_e (mg/g)	R_2^2
1.4×10^{-3}	16.26	0.92	1.95×10^{-4}	26.73	0.99

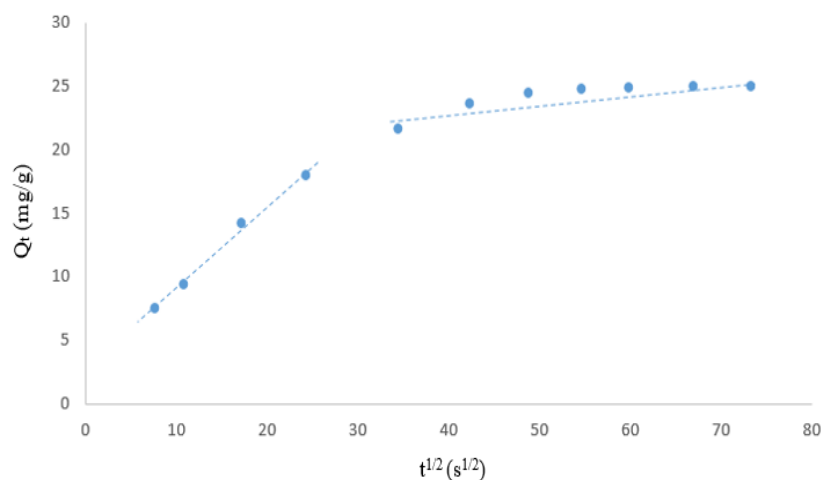
Moreover, to better explore the rate-limiting steps in the adsorption process the Webber-Morris model was employed. The Webber-Morris equation is as follows:

$$Q_t = k_i \sqrt{t} + C \quad i = [1, 2] \quad (4)$$

where Q_t is the capacity of the uptake of phosphate per one gram of the adsorbent after the time of t (mg/g), k_i is the rate constant parameter of the intra-particle diffusion model (mg/g min^{1/2}).

According to this model, if the graph is linear and passes through the origin, the only

rate-limiting step is the intra-particle diffusion; otherwise, other mechanisms are limiting the rate of the process. Figure 12 shows that a small deviation from the origin is present, revealing that the intra-particle diffusion is not the only step controlling the process rate. This deviation from the origin reveals that the adsorption of phosphate on the surface of IOAC might be an additional rate-limiting step. The second linear portion is assigned to the internal penetration of phosphate in IOAC.

**Figure 11.** Webber-Morris intra-particle diffusion model plot.

3.1.9. Adsorption isotherms

The influence of the concentration of phosphate on the adsorption process was investigated via batch experiments. In this regard, a 2 g/L IOAC was introduced to 50 mL of the phosphate solution at different concentrations. It was observed that the adsorption of phosphate increased by increasing the concentration of phosphate in

the solution, and then it reached equilibrium at higher concentrations. The equilibrium was reached as the available adsorption sites were saturated at higher concentrations. A quantitative analysis was performed using Langmuir and Freundlich isotherms. The equations are as follows:

$$\frac{C_e}{Q_e} = \frac{1}{Q_{\max} k_L} + \frac{C_e}{Q_{\max}} \quad (5)$$

$$\ln Q_e = \frac{1}{n} \ln C_e + \ln k_F \quad (6)$$

where Q_e is the amount of the removed phosphate at equilibrium per one gram of the adsorbent (mg/g), C_e is attributed to the concentration of phosphate at the equilibrium step (mg/L), k_L is the constant parameter of the Langmuir equation (L/mg), n is the linearity index, k_F is the constant parameter of the Freundlich equation (mg/g). Langmuir isotherm was much consistent with the data as the correlation coefficient for Langmuir isotherm was found to be larger than that for Freundlich isotherm. According to Langmuir isotherm, homogeneous and identical adsorption sites are available on the adsorbent and the monolayer adsorption of phosphate occurred during the process. The maximum phosphate removal capacity was also found to be 27.47 mg P/L. This result indicates the superior efficiency of IOAC in the elimination phosphate from an aqueous environment. The corresponding plots and

constant parameters are recorded in Figure 13, Figure 14 and Table 3.

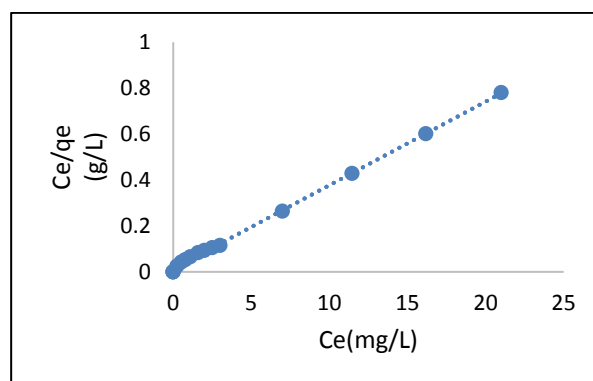


Figure 12. Langmuir isotherm plot.

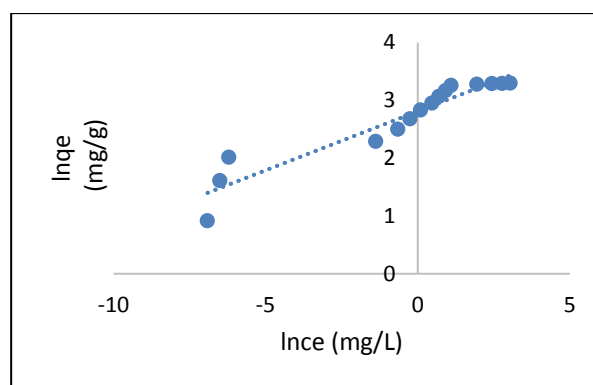


Figure 13. Freundlich isotherm plot.

Table 3

Fitting variables obtained from Langmuir and Freundlich isotherms.

Freundlich			Langmuir		
k_F (mg/g)	n	R_F^2	k_L (L/mg)	Q_{max} (mg/g)	R_L^2
16.61	4.89	0.90	2.71	27.47	0.99

4. Conclusions

This study has investigated the preparation of iron oxide/activated carbon composites based on a novel raw material for the elimination of phosphate from the water environment. The modification of iron oxide was followed to improve the removal of phosphate and facilitate the separation of the adsorbent from the mixture. While many adsorbents need special processes to be removed from the aqueous solution, IOAC was removed from the mixture via a simple magnetic process.

The maximum phosphate removal using IOAC was achieved as large as 27 mg/g, approximately twice the removal capacity achieved by similar activated carbon derived from biomasses. Also, IOAC showed fast adsorption kinetics, achieving equilibrium in only 60 minutes. Moreover, the specific surface area for IOAC reached 569.41 m²/g, comparable to that of the commercial activated carbon. However, further research is needed to investigate the increase in the surface area. We suggest optimizing the

preparation conditions, including the carbonization time, carbonization temperature and amount of the chemical reagent with the objective of the largest specific surface area.

Acknowledgement

Authors wish to thank Petroleum University of Technology for the work space and instrumental facilities.

References

- [1] Bahramian, A., "Hazards identification and the units assessment of a the water treatment plant against pathogenic and biotoxin threats affecting by physicochemical parameters," *Iranian Journal of Chemical Engineering (IJChE)*, **17** (4), 33 (2020).
- [2] Goscianska, J., Ptaszkowska-Koniarz, M., Frankowski, M., Franus, M., Panek, R. and Franus, W., "Removal of phosphate from water by lanthanum-modified zeolites obtained from fly ash", *J. Colloid Interface Sci.*, **513**, 72 (2018).
- [3] Conley, D. J., Paerl, H. W., Howarth, R. W., Boesch, D. F., Seitzinger, S. P., Karl E, K. E., Lancelot, C. and Gene E, G. E., "Controlling eutrophication: Nitrogen and phosphorus", *Science*, **123**, 1014 (2009).
- [4] Wang, J., Chen, J., Jin, Z., Guo, J., Yang, H., Zeng, Y. and Liu, Y., "Simultaneous removal of phosphate and ammonium nitrogen from agricultural runoff by amending soil in lakeside zone of Karst area, Southern China", *Agric. Ecosyst. Environ.*, **289**, 106745 (2020).
- [5] Ye, Y., Ngo, H. H., Guo, W., Liu, Y., Li, J., Liu, Y., Zhang, X. and Jia, H., "Insight into chemical phosphate recovery from municipal wastewater", *Sci. Total Environ.*, **576**, 159 (2017).
- [6] Karaca, S., Gürses, A., Ejder, M. and Açıkyıldız, M., "Kinetic modeling of liquid-phase adsorption of phosphate on dolomite", *J. Colloid Interface Sci.*, **277** (2), 257 (2004).
- [7] Singh, M. and Srivastava, R., "Sequencing batch reactor technology for biological wastewater treatment: A review", *Asia-Pacific Journal of Chemical Engineering*, **6** (1), 3 (2011).
- [8] Yao, Y., Gao, B., Inyang, M., Zimmerman, A. R., Cao, X., Pullammanappallil, P. and Yang, L., "Removal of phosphate from aqueous solution by biochar derived from anaerobically digested sugar beet tailings", *J. Hazard. Mater.*, **190** (1-3), 501 (2011).
- [9] Clark, T., Stephenson, T. and Pearce, P., "Phosphorus removal by chemical precipitation in a biological aerated filter", *Water research*, **31** (10), 2557 (1997).
- [10] Özacar, M., "Adsorption of phosphate from aqueous solution onto alunite", *Chemosphere*, **51** (4), 321 (2003).
- [11] Foletto, E. L., Weber, C. T., Paz, D. S., Mazutti, M. A., Meili, L., Bassaco, M. M. and Collazzo, G. C., "Adsorption of leather dye onto activated carbon prepared from bottle gourd: equilibrium, kinetic and mechanism studies", *Water Sci. Technol.*, **67** (1), 201 (2013).
- [12] Mohammadi, N., Mousazadeh, B. and Hamoule, T., "Synthesis and characterization of NH₂-SiO₂@ Cu-MOF as a high-performance adsorbent for Pb ion removal from water environment", *Environment, Development and Sustainability*, **23** (58), 1688 (2021).
- [13] Jahanban-Esfahlan, A., Jahanban-Esfahlan, R., Tabibiazar, M.,

- Roufegarinejad, L. and Amarowicz, R., "A Review on the hazardous materials removal using activated carbons derived from walnut (*Juglans regia* L.) shell", *Iranian Journal of Chemical Engineering (IJChE)*, **17** (1), 3 (2020).
- [14] Hu, J., Zhao, D. and Wang, X., "Removal of Pb (II) and Cu (II) from aqueous solution using multiwalled carbon nanotubes/iron oxide magnetic composites", *Water Sci. Technol.*, **63** (5), 917 (2011).
- [15] Abdelrahman, E. A., Abou El-Reash, Y., Youssef, H. M., Kotp, Y. H. and Hegazey, R., "Utilization of rice husk and waste aluminum cans for the synthesis of some nanosized zeolite, zeolite/zeolite, and geopolymer/zeolite products for the efficient removal of Co (II), Cu (II), and Zn (II) ions from aqueous media", *J. Hazard. Mater.*, **401**, 123813 (2021).
- [16] Ghasemi, M., Ghoreyshi, A., Younesi, H. and Khoshhal, S. K., "Synthesis of a high characteristics activated carbon from walnut shell for the removal of Cr (VI) and Fe (II) from aqueous solution: Single and binary solutes adsorption", *Iranian Journal of Chemical Engineering (IJChE)*, **12** (4), 28 (2015).
- [17] Haichao, L., Shou-Xin, L. and Shi-Run, Z., "Preparation of high yield nutshell activated carbon", *J. Forestry Science and Technology*, **5**, 42 (2001).
- [18] Annadurai, G., Juang, R. -S. and Lee, D., "Adsorption of heavy metals from water using banana and orange peels", *Water Sci. Technol.*, **47** (1), 185 (2003).
- [19] Yao, Y., Gao, B., Inyang, M., Zimmerman, A. R., Cao, X., Pullammanappallil, P. and Yang, L., "Biochar derived from anaerobically digested sugar beet tailings: Characterization and phosphate removal potential", *Bioresour. Technol.*, **102** (10), 6273 (2011).
- [20] Ju, X., Hou, J., Tang, Y., Sun, Y., Zheng, S. and Xu, Z., "ZrO₂ nanoparticles confined in CMK-3 as highly effective sorbent for phosphate adsorption", *Microporous and Mesoporous Materials*, **230**, 188 (2016).
- [21] Xiong, W., Tong, J., Yang, Z., Zeng, G., Zhou, Y., Wang, D., Song, P., Xu, R., Zhang, C. and Cheng, M., "Adsorption of phosphate from aqueous solution using iron-zirconium modified activated carbon nanofiber: Performance and mechanism", *J. Colloid Interface Sci.*, **493**, 17 (2017).
- [22] Zhang, L., Zhou, Q., Liu, J., Chang, N., Wan, L. and Chen, J., "Phosphate adsorption on lanthanum hydroxide-doped activated carbon fiber", *Chemical Engineering Journal*, **185**, 160-167 (2012).
- [23] Zahoor, M. and Ali Khan, F., "Aflatoxin B1 detoxification by magnetic carbon nanostructures prepared from maize straw", *Desalination and Water Treatment*, **57** (25), 11893 (2016).
- [24] Nasiruddin Khan, M. and Sarwar, A., "Determination of points of zero charge of natural and treated adsorbents", *Surface Review and Letters*, **14** (03), 461 (2007).
- [25] Huang, W., Li, D., Zhu, Y., Xu, K., Li, J., Han, B. and Zhang, Y., "Fabrication of Fe-coordinated diamino-functionalized SBA-15 with hierarchical porosity for phosphate removal", *Materials Letters*, **99**, 154 (2013).